Determination of Interconversion Barriers by Dynamic Gas Chromatography: Epimerization of Chalcogran

Oliver Trapp and Volker Schurig*[a]

Abstract: The four stereoisomers of chalcogran **1** ((2*RS*,5*RS*)-2-ethyl-1,6-dioxaspiro[4.4]nonane), the principal component of the aggregation pheromone of the bark beetle pityogenes chalcographus, are prone to interconversion at the spiro center (C5). During diastereo- and enantioselective dynamic gas chromatography (DGC), epimerization of **1** gives rise to two independent interconversion peak profiles, each featuring a plateau between the peaks of the interconverting epimers. To determine the rate constants of epimerization by dynamic gas chromatography (DGC), equations to simulate the complex elution profiles were derived, using the theoretical plate model and the stochastic model of the chromatographic process. The Eyring activation parameters of the experimental interconversion profiles, between 70 and 120 °C in the presence of the chiral stationary phase (CSP) Chirasil-β-Dex, were then determined by computer-aided simulation with the aid of the new program ChromWin: (2*R*,5*R*)-**1**: $\Delta G^{\neq}(298.15\ \mathrm{K}) = 108.0 \pm 0.5\ \mathrm{kJ\,mol^{-1}}$, $\Delta H^{\neq} = 47.1 \pm 0.2\ \mathrm{kJ\,mol^{-1}}$, $\Delta S^{\neq} = -204 \pm 6\ \mathrm{J\,K^{-1}\,mol^{-1}}$; (2*R*,5*S*)-**1**: $\Delta G^{\neq}$ (298.15 K) $= 108.5 \pm 0.5\ \mathrm{kJ\,mol^{-1}}$, $\Delta H^{\neq} = 45.8 \pm 0.2\ \mathrm{kJ\,mol^{-1}}$, $\Delta S^{\neq} = -210 \pm 6\ \mathrm{J\,K^{-1}\,mol^{-1}}$; (2*S*,5*S*)-**1**: $\Delta G^{\neq}$ (298.15 K) $= 108.1 \pm 0.5\ \mathrm{kJ\,mol^{-1}}$, $\Delta H^{\neq} = 49.3 \pm 0.3\ \mathrm{kJ\,mol^{-1}}$, $\Delta S^{\neq} = -197 \pm 8\ \mathrm{J\,K^{-1}\,mol^{-1}}$; (2*S*,5*R*)-**1**: $\Delta G^{\neq}$ (298.15 K) $= 108.6 \pm 0.5\ \mathrm{kJ\,mol^{-1}}$, $\Delta H^{\neq} = 48.0 \pm 0.3\ \mathrm{kJ\,mol^{-1}}$, $\Delta S^{\neq} = -203 \pm 8\ \mathrm{J\,K^{-1}\,mol^{-1}}$. The thermodynamic Gibbs free energy of the *E*/*Z* equilibrium of the epimers was determined by the stopped-flow multidimensional gas chromatographic technique: $\Delta G_{E/Z}$ (298.15 K) $= -0.5\ \mathrm{kJ\,mol^{-1}}$, $\Delta H_{E/Z} = 1.4\ \mathrm{kJ\,mol^{-1}}$ and $\Delta S_{E/Z} = 6.3\ \mathrm{J\,K^{-1}\,mol^{-1}}$. An interconversion pathway proceeding through ring-opening and formation of a zwitterion and an enol ether/alcohol intermediate of **1** is proposed.

Keywords: ChromWin · gas chromatography · epimerization barrier · kinetics · spiro compounds

Introduction

Spiroketals are an important class of chiral compounds, widely distributed in nature as microbial metabolites such as reveromycins, which show a potent antiproliferative activity against certain human tumor cells,[1, 2] ionophore antibiotics such as calcimycin (A-23187) from *Streptomyces chartreusensis* (L.) and routiennocin from *Streptomyces routiennii* (L.),[3] cell growth inhibitors such as the cephalostatines from the South African sea worm *Cephalodiscus gilchristi* (L.),[4] steroids in *Solanaceae* (L.), such as diosgenin, yamogenin, hecogenin, and willagenin,[5] highly toxic metabolites calyculinene A, B and C of the marine sponge *Discodermis calyx* (L.),[6] marine macrolide spongistatine 1[7], marine toxins such as pinnatoxins,[8] and as volatile pheromones for communication between insects.[9] Francke et al.[10] isolated chalcogran **1** ((2*RS*,5*RS*)-2-ethyl-1,6-dioxaspiro[4.4]nonane (Figure 1), the principal component of the aggregation pheromone of the bark beetle *Pityogenes chalcographus* (L.), a pest of the Norway spruce.

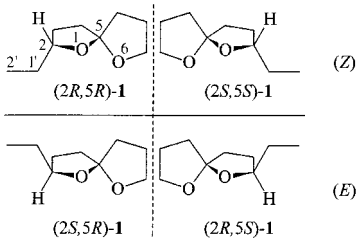

Figure 1. Epimeric and enantiomeric pairs of chalcogran. Top left: (*Z*)-(2*R*,5*R*)-2-ethyl-1,6-dioxaspiro[4.4]nonane: (2*R*,5*R*)-**1**. Top right: (*Z*)-(2*S*,5*S*)-2-ethyl-1,6-dioxaspiro[4.4]nonane: (2*S*,5*S*)-**1**. Bottom left: (*E*)-(2*S*,5*R*)-2-ethyl-1,6-dioxaspiro[4.4]nonane: (2*S*,5*R*)-**1**. Bottom right: (*E*)-(2*R*,5*S*)-2-ethyl-1,6-dioxaspiro[4.4]nonane: (2*R*,5*S*)-**1**.

The structure of **1** was confirmed by synthesis of the racemic mixture[10, 11] of the *E*/*Z* epimer pairs and the absolute configuration was assigned by stereoselective synthesis.[12]

The role of chirality in pheromone perception is well established,[13, 14] and the quantitative analytical separation of

[a] Prof. Dr. V. Schurig, Dipl.-Chem. O. Trapp
Institut für Organische Chemie, Universität Tübingen
Auf der Morgenstelle 18, 72076 Tübingen (Germany)
Fax: (+49) 7071-29-5538
E-mail: volker.schurig@uni-tuebingen.de

stereoisomers is a prerequisite for identification of the biologically active stereoisomer and the development of suitable methods for insect control.[15] The first separation and chromatographic assignment of all four stereoisomers of **1** was achieved by enantioselective complexation chromatography employing the chiral stationary phase (CSP) nickel(II)-bis[(1*R*)-6-(heptafluorobutanoyl)-pulegonate].[16–18] At increased separation temperatures, overlapping interconversion peak profiles, featuring a plateau between the peaks of the epimers, were observed on the chiral stationary phases nickel(II)-bis[(1*R*)-6-(heptafluorobutanoyl)-pulegonate],[16, 17] nickel(II)-bis[(1*R*)-3-(heptafluorobutanoyl)-camphorate],[17b, 19] heptakis(2,6-di-*O*-methyl-3-*O*-trifluoroacetyl)-β-cyclodextrin,[20] and hexakis(6-*O*-methyl-2,3-di-*O*-pentyl)-α-cyclodextrin.[21] This was attributed to interconversion of the four stereoisomers occurring during separation.[22] The low stereostability of the spiroketal functionality, which was also corroborated by synthetic investigations,[23] commands heightened interest in view of the diversity of spiroketals in nature.

In this study, we applied diastereo- and enantioselective dynamic gas chromatography (DGC) to **1** and, using the theoretical plate model and the stochastic model of chromatography, derived mathematical equations which, for the first time, allow the determination of epimerization barriers for both enantiomeric pairs by dynamic chromatography. This general method, described below, may also be employed for many current problems in dynamic chromatographic experiments, such as *E*/*Z* isomerism of hydrazones, imines, and oximes,[24] interconversion of dipeptide conformers[25] and phenanthrene derivatives,[26] stereoisomerism of organic metal complexes.[27]

Abstract in German: *Die vier Stereoisomere des Chalcograns **1** ((2RS,5RS)-2-Ethyl-1,6-dioxaspiro[4.4]nonan), der Hauptkomponente des Aggregatiospheromons des Fichtenborkenkäfers Pityogenes chalcographus, epimerisieren am Spirokohlenstoffatom (C5). Diastereo- und enantioselective dynamische Gaschromatographie (DGC) von **1** zeigt zwei voneinander unabhängige Umwandlungsprofile, die durch das Auftreten von Plateaus zwischen den Peaks der gegenseitig umwandelnden Epimeren charakterisiert sind. Zur Bestimmung der Geschwindigkeitskonstanten der Epimerisierung mittels dynamischer Gaschromatographie (DGC) wurden Gleichungen hergeleitet, die eine Simulation solcher Elutionsprofile mit dem theoretischen Bödenmodel und dem stochastischen Model erlauben. Die Aktivierungsparameter $\Delta H^{\neq}$ und $\Delta S^{\neq}$ wurden mit dem neuen Programm ChromWin durch Computersimulation der experimentellen Chromatogramme zwischen 70 und 120 °C in Gegenwart der chiralen Stationärphase (CSP) Chirasil-β-Dex erhalten. Die Gibbsche freie Enthalpie $\Delta G_{E/Z}$ des E/Z Gleichgewichts der Epimere wurde mit stopped-flow multidimensionaler Gaschromatographie bestimmt. Für die Epimerisierung wird eine Ringöffnung unter Bildung eines Zwitterions und eines Enolether/ Alkohol-Intermediates von **1** vorgeschlagen.*

Results and Discussion

In diastereo- and enantioselective dynamic gas chromatography (DGC), molecular interconversion—that is, enantiomerization[28] and epimerization,[29] respectively—gives rise to an interconversion peak profile featuring a plateau between the terminal peaks or peak broadening,[30, 31] evident in the tailing of the first peak and fronting of the second peak, of the corresponding stereoisomers. If it is possible to separate both epimeric pairs into their enantiomers on a chiral stationary phase (CSP) by gas chromatography, the two epimerization processes $A_{RR} \rightleftharpoons B_{RS}$ and $A_{SS} \rightleftharpoons B_{SR}$ can be observed independently.

If peak form analysis is used, kinetic data of interconversion can be obtained by iterative comparison of experimental and simulated chromatograms.[32–34] The application of the principle of microscopic reversibility requires that the rates of interconversion of the corresponding stereoisomers be different in the presence of the chiral stationary phase (CSP). This phenomenon arises from the fact that the stereoisomers are discriminated, and hence separated, by means of a different thermodynamic Gibbs energy ($-\Delta_{B,A}\Delta G = RT \ln(K_B/K_A)$), as shown in Scheme 1.

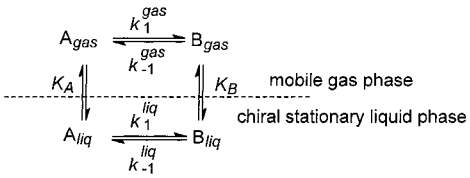

Scheme 1. Equilibria in a theoretical plate of a gas chromatographic column: A is the stereoisomer eluted first, B is the stereoisomer eluted second, *k* represents the rate constant and *K* the distribution constant. The index *liq* represents the stationary liquid phase and *gas* the mobile gas phase.

Thus, whereas the stereoisomer B, eluted second, is enriched during the chromatographic separation timescale, because it is formed more rapidly than the first eluted stereoisomer A ($k_1^{liq} > k_{-1}^{liq}$), no displacement of the equilibrium between A and B occurs at constant temperature, since the second eluted stereoisomer B is depleted to a greater extent due to its longer residence time on the column.

The prerequisite for the technique of dynamic chromatography is the quantitative, on-column separation of the diastereomeric mixture into the four stereoisomers on a chiral stationary phase (CSP), in the respective chromatographic setup. The four stereoisomers of **1** can indeed be separated by enantioselective gas chromatography on Chirasil-β-Dex[35] (permethylated β-cyclodextrin linked by a monooctamethylene spacer to polydimethylsiloxane). The elution order of **1** on Chirasil-β-Dex,[35] determined by coinjection of enantiomerically enriched (2*S*,5*RS*)-**1** and taking into account the preponderance of the energetically favorable ((2*R*,5*S*)-**1** and (2*S*,5*R*)-**1**)) *E* diastereomers, is (2*R*,5*S*)-**1**, (2*R*,5*R*)-**1**, (2*S*,5*S*)-**1**, and (2*S*,5*R*)-**1**.

When subjected to increases in temperature, from 70 to 120 °C, chalcogran **1** shows typical interconversion plateaus between the epimers (2*R*,5*S*)-**1**/(2*R*,5*R*)-**1** and (2*S*,5*S*)-**1**/(2*S*,5*R*)-**1** (Figure 2), which implies that the epimerization process, as expected, takes place only at the spiro center (C5).

0947-6539/01/0707-1496 $ 17.50+.50/0 *Chem. Eur. J.* **2001**, *7*, No. 7

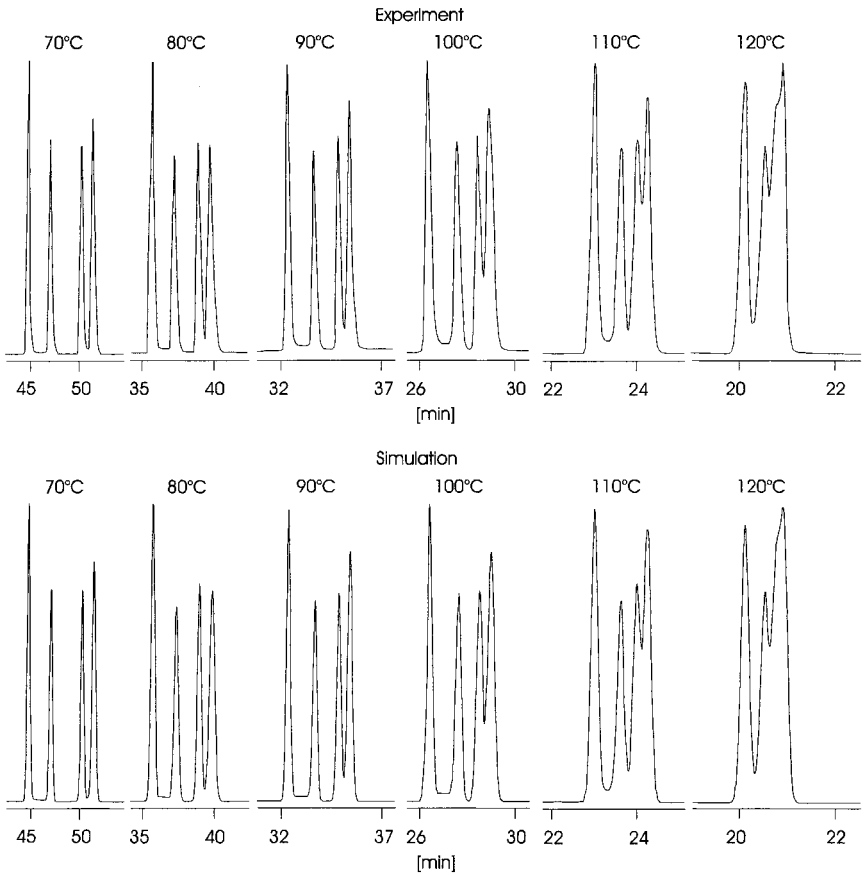

Figure 2. Epimerization of **1** at different temperatures: experimental chromatograms (top) versus simulated chromatograms (bottom).

The rate constants were calculated by simulation of the chromatograms using the new program ChromWin,[34] which permits calculation with the theoretical plate model (TPM),[30, 32, 34] the stochastic model (SM),[36, 37] and the modified "stochastic model plus" (SM+).[34]

The theoretical plate model describes the chromatographic separation as a discontinuous process, assuming that all steps proceed repeatedly in uniform sections of a multicompartmental column with N theoretical plates considered as chemical reactors. Three steps i) to iii) take place in every plate (Scheme 1): i) distribution (partitioning) of the stereoisomers A and B between the mobile gas phase (*gas*) and the stationary liquid phase (*liq*), ii) reversible interconversion between A and B during the residence time Δt, calculated from the hold-up time t_M and the number of plates N according to $\Delta t = t_M/N$, and iii) shifting of the content of the mobile phase to the subsequent theoretical plate. While the given amount of the enantiomers is initially introduced into the first theoretical plate, the content of the mobile phase of the last theoretical plate is finally recorded as a chromatogram featuring an interconversion profile over the time t.

Unlike enantiomerization processes, for which the rate constants of the forward and backward reactions are equal in the achiral gas phase, step ii) is more complicated for epimerization processes, because of the different ground state energies of epimers. This results in different rate constants and different initial quantities for the epimers in the mobile gas and stationary liquid phases.

The ratio of forward and backward rate constants of the mobile gas phase depends on the equilibrium of the epimers A and B according to Equation (1).

$$K^{gas} = \frac{k_1^{gas}}{k_{-1}^{gas}} = \frac{[B]}{[A]} \quad (1)$$

The equilibrium constant K^{liq} in the chiral stationary phase depends on the two phase distribution constants (= partition coefficients) K_A and K_B, according to the principle of microscopic reversibility (Scheme 1):[30]

$$K^{liq} = \frac{K_B}{K_A} = \frac{k_B'}{k_A'} = \frac{k_1^{liq}}{k_{-1}^{liq}} \frac{k_{-1}^{gas}}{k_1^{gas}} \quad (2)$$

This implies that the backward rate constant k_{-1}^{liq} is already determined for given values of k_1^{liq}, the ratio of [A] to [B] and the retention factors k_A' and k_B', calculated from the total retention time t_R and the mobile phase hold-up time t_M according to $k' = (t_R - t_M)/t_M$.

$$k_{-1}^{liq} = \frac{k_A'}{k_B'} k_1^{liq} \frac{[A]}{[B]} \quad (3)$$

However, from the computer simulation of the elution profiles of the DGC experiment it is not possible to differentiate between the rate constants in the mobile gas and in the stationary liquid phase. Only apparent rate constants (k_1^{app} and k_{-1}^{app}), which are mean averages of the forward and backward rate constants of the mobile and stationary phase, weighted by the retention factors k_A' and k_B', can be determined. Taking into account that the backward reaction rate can be calculated from the forward reaction rates and the equilibrium constant between A and B, the following equations were derived:

$$k_1^{app} = \frac{1}{1+k_A'} k_1^{gas} + \frac{k_A'}{1+k_A'} k_1^{liq}$$

$$k_{-1}^{app} = \frac{[A]}{[B]} \left(\frac{1}{1+k_B'} k_1^{gas} + \frac{k_B'}{1+k_B'} \frac{k_A'}{k_B'} k_1^{liq} \right) \quad (4)$$

In the case in which the rate constants in the mobile gas and stationary liquid phase are equal to a first approximation ($k_1^{gas} = k_1^{liq}$; $k_{-1}^{gas} = k_{-1}^{liq}$), the apparent rate constants (k_1^{app} and k_{-1}^{app}) are given by:

$$k_1^{app} = k_1^{gas} = k_1^{liq}$$
$$k_{-1}^{app} = k_{-1}^{gas} = k_{-1}^{liq} \quad (5)$$

If the rate constants in the gas phase are accessible by an independent method, it is possible to calculate the rate constants in the stationary liquid phase, as previously described.[34]

The equations derived here can also be applied to the stochastic model for the calculation of elution profiles by a probability distribution function.[31, 34b, 36] Differences between these two models are illustrated in Figure 3 for the epimerization of **1** at 90 °C.

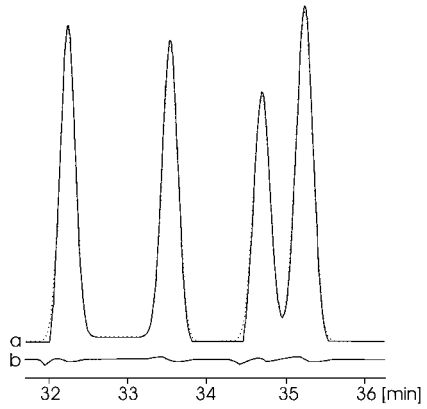

Figure 3. a) Comparison of simulated elution profiles of **1** by the theoretical plate model (TPM; plain line) and the stochastic model plus (SM+; top: dotted line). b) Represents the difference between the two models (TPM − SM+). Data from the DGC experiment at 90 °C and a mean plate number N of 100 000 were used for simulation.

To evaluate the chromatograms of **1** obtained by the DGC experiment, it is necessary to determine quantitatively the temperature-dependent thermodynamic equilibrium ratio of the epimers between 70 and 120 °C. As peak overlapping occurs at higher temperatures, the use of E/Z equilibrium ratios from the DGC experiment is inaccurate. Therefore, the stopped-flow multidimensional gas chromatographic technique (sfMDGC),[34, 38] originally developed for the determination of enantiomerization barriers in the inert gas phase, was employed as follows.

The gas chromatograph is equipped with two ovens, a pneumatically controlled six-port valve (Valco), with valve positions A and B, two flame-ionization detectors (FID 1 and FID 2), two separation columns (column 1 and 3) and a reaction column (column 2). In valve position A, injector 1, column 1 and FID 1 are connected, the reaction column 2 is closed, and injector 2, column 3 and FID 2 are connected. In valve position B, injector 1, column 1, reaction column 2, column 3 and FID 2 are in line and injector 2 is directly connected to FID 2. The diastereomeric mixture of **1** is quantitatively separated in column 1 (Chirasil-β-Dex)[35] in the first oven, in valve position A, at 60 °C.

Afterwards, either the first ((2*R*,5*S*)-**1**/(2*R*,5*R*)-**1**) or the second ((2*S*,5*S*)-**1**/(2*S*,5*R*)-**1**) pair of epimers is trapped in reaction column 2 in the second oven, via valve position B. The unique elution order of the stereoisomers ((2*R*,5*S*)-**1** < (2*R*,5*R*)-**1** < (2*S*,5*S*)-**1** < (2*S*,5*R*)-**1**) permits the experiment to be carried out for both epimeric pairs, which are enantiomeric to each other. For that purpose reaction column 2 is cooled with liquid nitrogen. Reactor column 2, deactivated with polydimethylsiloxane (1 m × 0.25 mm i.d., 0.002 μm), is quickly heated to temperature T in valve position A, whereby equilibration of either (2*R*,5*S*)-**1**/(2*R*,5*R*)-**1** or (2*S*,5*S*)-**1**/(2*S*,5*R*)-**1**, respectively, commences. After the contact time t, reaction column 2 is rapidly cooled down with liquid nitrogen and the epimeric mixture of **1** is transferred at the separation temperature into column 3, in valve position B, where the epimers of **1** are separated on Chirasil-β-Dex. The equilibrium ratio $K_{E/Z}$ and the Gibbs free energy $\Delta G_{E/Z}$ are calculated from the peak areas (Table 1). Side products from decomposition or rearrangement, if any, were not observed.

Table 1. Temperature-dependent determination of the epimer equilibrium by the stopped-flow MDGC experiment. The major peak area represents the (2*R*,5*S*)-**1** and (2*S*,5*R*)-**1** diastereomers, respectively. $K_{E/Z}$ denotes the equilibrium constant, defined as the ratio of major to minor peak area.

T [°C]	Major peak area [%]	$K_{E/Z}$	$\Delta G_{E/Z}$ [kJ mol^{-1}]
70.0	57.0	1.32	− 0.80
80.0	57.3	1.34	− 0.86
90.0	57.6	1.36	− 0.92
100.0	57.9	1.37	− 0.98
110.0	58.2	1.39	− 1.05
120.0	58.5	1.41	− 1.12

The mean values of $-\Delta G_{E/Z}$ were plotted as function of T^{-1}, and from the linear regression (agreement factor $r^2 = 0.9994$) $\Delta H_{E/Z}$ was found to be 1.4 kJ mol^{-1} and $\Delta S_{E/Z} = 6.3$ J K mol^{-1} in the gas phase.

With these data and Equation (4), the apparent rate constants of the forward and backward reaction (k_1^{app}, k_{-1}^{app}) for each pair of epimers (2*R*,5*S*)-**1**/(2*R*,5*R*)-**1**) and (2*S*,5*S*)-**1**/(2*S*,5*R*)-**1**) were determined by computer simulation of the experimental chromatograms of the DGC experiment between 70 and 110 °C (Table 2). Since strong overlapping arose

Table 2. Selected experimental data and rate constants for the epimerization of **1**, obtained using ChromWin on the basis of the modified stochastic model (SM+).

T [°C]	t_M	t_R[a]	t_R[b] [min]	t_R[c]	t_R[d]	N[a]	N[b]	N[c]	N[d]	$k_{a\to b}^{app}$	$k_{b\to a}^{app}$ [1×10^{-5} s^{-1}]	$k_{c\to d}^{app}$	$k_{d\to c}^{app}$
70	2.68	45.20	47.34	50.33	51.45	112 000	117 150	117 100	111 950	0.83	1.10	1.10	0.83
80	3.39	35.54	37.18	38.85	39.65	69 400	61 450	61 450	69 400	1.52	2.03	1.85	1.38
90	4.66	32.23	33.53	34.69	35.24	102 550	98 550	98 500	102 550	2.14	2.90	3.10	2.28
100	5.76	27.25	28.19	28.85	29.23	83 350	85 900	85 950	83 300	3.57	4.89	5.00	3.64
110	6.56	22.96	23.60	23.98	24.24	63 250	58 250	63 250	58 250	4.80	6.68	7.31	5.26

[a] (2*R*,5*S*)-**1**. [b] (2*R*,5*R*)-**1**. [c] (2*S*,5*S*)-**1**. [d] (2*S*,5*R*)-**1**. t_M: mobile phase hold-up time, measured from the (essentially unretained) methane peak.[39] t_R: total retention time of the single stereoisomers. N: number of theoretical plates calculated by ChromWin.

0947-6539/01/0707-1498 $ 17.50+.50/0 *Chem. Eur. J.* **2001**, *7*, No. 7

in the chromatograms of the later eluted epimeric pair (2*S*,5*S*)-**1**/(2*S*,5*R*)-**1** at 120 °C, these values have not been considered for the calculation of the activation parameters.

The mean values of ln(k/T) were plotted as a function of T^{-1} according to the Eyring equation (Figure 4). The activation parameters evaluated by a linear regression of the Eyring plots (agreement factor: (2*R*,5*S*)-**1**/(2*R*,5*R*)-**1**: $r^2 = 0.996$; (2*S*,5*S*)-**1**/(2*S*,5*R*)-**1**: $r^2 = 0.999$) are represented in Table 3.

The activation parameters $\Delta G^{\neq}$, ΔH^{+}, and ΔS^{+} for the pairs of enantiomers (2*R*,5*R*)-**1**/(2*S*,5*S*)-**1** and (2*R*,5*S*)-**1**/(2*S*,5*R*)-**1** show the same tendency—the first eluted epimer has a higher activation enthalpy and a lower activation entropy compared to the later eluted epimer. The activation enthalpies ΔH^{+} increase for the later eluted epimers, which could be interpreted as a stronger interaction with the chiral stationary phase (CSP) and stabilization of the analyte.

The low experimental activation enthalpy ΔH^{+} and the highly negative activation entropy ΔS^{+} observed for all four stereoisomers may be considered as an evidence for a dissociative mechanism of the inversion process. The increase in the negative entropy is characteristic for charge separation in heterolytic processes,[40] but not for homolytic processes.[41] As already pointed out, it is necessary that C5 in **1** be sp^2-hybridized and hence planar for the transition state of interconversion.

From these results, a mechanism of interconversion of **1** by bond breakage of O1–C5 or C5–O6 at the spiro center C5 and formation of a zwitterion/enol ether/alcohol structure, which can be stabilized by a proton shift as a very reactive enol ether alcohol intermediate, can tentatively be envisaged (Figure 5).

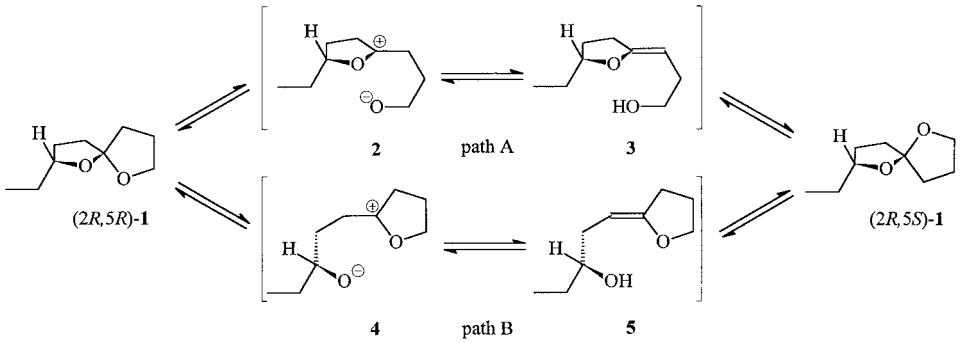

Figure 5. Proposed mechanism of interconversion of the epimeric pair (2*R*,5*R*)-**1**/(2*R*,5*S*)-**1** via a zwitterion/enol ether/alcohol intermediate.

For the enantiomerization of structurally related spirobinaphthopyrans and spirochromenes, Mannschreck et al.[42] and Okamoto et al.[43] also proposed acyclic intermediates, which are stabilized by the extended π-system, therefore lowering the enantiomerization barrier $\Delta G^{\neq}$ to about 85–105 kJ mol^{-1}. Unfortunately, no activation parameters were determined by temperature-dependent measurement to support this mechanism.

To corroborate the mechanism depicted in Figure 5, optimized structures of (2*R*,5*R*)-**1** and (2*R*,5*S*)-**1** (Figure 6; the energies of the enantiomers are the same) were calculated with the HyperChem Package release 4.0[44] using the MM+ force field[45] followed by the PM3 method.[46] To find the

Table 3. Activation parameters of **1** from the DGC experiment.

	$\Delta G^{\neq}$(298.15 K) [kJ mol^{-1}]	ΔH^{+} [kJ mol^{-1}]	ΔS^{+} [J K^{-1} mol^{-1}]
(2*R*,5*R*)-**1**	108.0 ± 0.5	47.1 ± 0.2	− 204 ± 6
(2*S*,5*S*)-**1**	108.1 ± 0.5	49.3 ± 0.3	− 197 ± 8
(2*R*,5*S*)-**1**	108.5 ± 0.5	45.8 ± 0.2	− 210 ± 6
(2*S*,5*R*)-**1**	108.6 ± 0.5	48.0 ± 0.3	− 203 ± 8

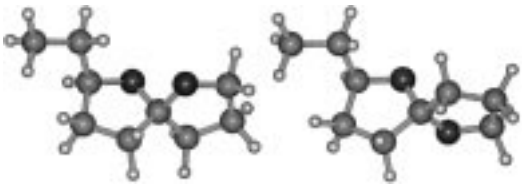

Figure 6. PM3-optimized structures. Left: (2*R*,5*R*)-**1**. Right: (2*R*,5*S*)-**1**.

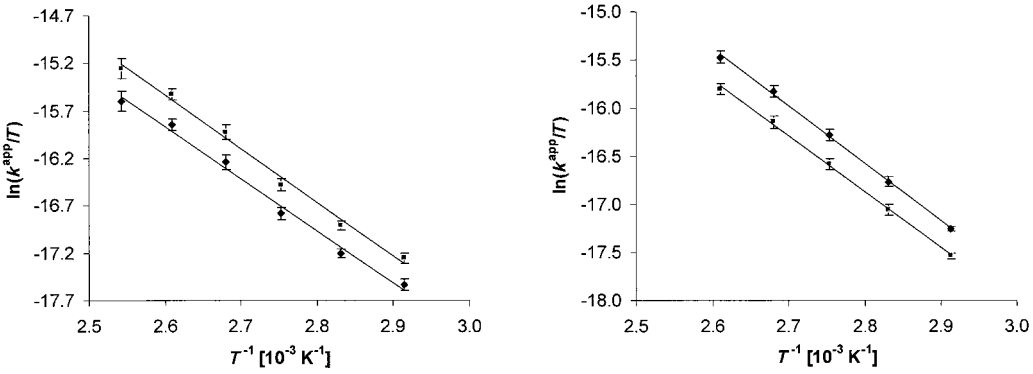

Figure 4. Eyring plot for the determination of ΔH^{+} and ΔS^{+} from the DGC experiment. Left: (2*R*,5*S*)-**1** (◆)/(2*R*,5*R*)-**1** (■). Right: (2*S*,5*S*)-**1** (◆)/(2*S*,5*R*)-**1** (■).

favorable conformation, the torsion angle O1–C2–C1′–C2′ was varied in 10° steps from −180° to 180°, and the structures obtained were geometrically optimized by the PM3 method. The local minima were again geometrically optimized without any restraints. The optimum found for (2*R*,5*R*)-**1** and (2*R*,5*S*)-**1** was at a torsion angle of about 180°. The relative energy difference ΔE between these structures is about 0.9 kJ mol^{-1} and is within the error range of semiempirical calculation in accordance with the experimental value, as expected for the *E*/*Z* isomers.

In a second step, the bonds O1–C5 and C5–O6 in (2*R*,5*R*)-**1** were broken and the atoms O1–C4–C5–C9 and C4–C5–O6–C9, respectively, were constrained to a planar sp^2-hybridized C5 atom geometry. The resulting structures **2** and **4** were optimized by the MM+ force field followed by the PM3 method. Additionally, the strongly acidic protons at C4 and C9, respectively, were removed, a double bond was formed between C4–C5 and C5–C9, respectively, and the alkoxy groups were protonated. The resulting enol ether/alcohol structures **3** and **5** constitute the *E*/*Z* isomers (*E*)-**3**, (*Z*)-**3**, (*E*)-**5**, and (*Z*)-**5**, respectively, and were optimized by the MM+ force field followed by the PM3 method. The results are depicted in Figure 7 and the energies calculated by the PM3 method are listed in Table 4.

The difference in the total energies of (2*R*,5*S*)-**1** and the structures **2** and **4** is about 170 kJ mol^{-1}. The structures **2** and **4** can be stabilized as reactive enol ether/alcohol intermediates **3** and **5**, which undergo ring-closure through an intramolecular enol ether/alcohol addition. In this case the intermediates (*E*)-**3** and (*Z*)-**3** are energetically favored relative to (*E*)-**5** and (*Z*)-**5** ($\Delta\Delta E \approx 8$ kJ mol^{-1}), and therefore reaction path A (cf. Figure 5) should be preferred.

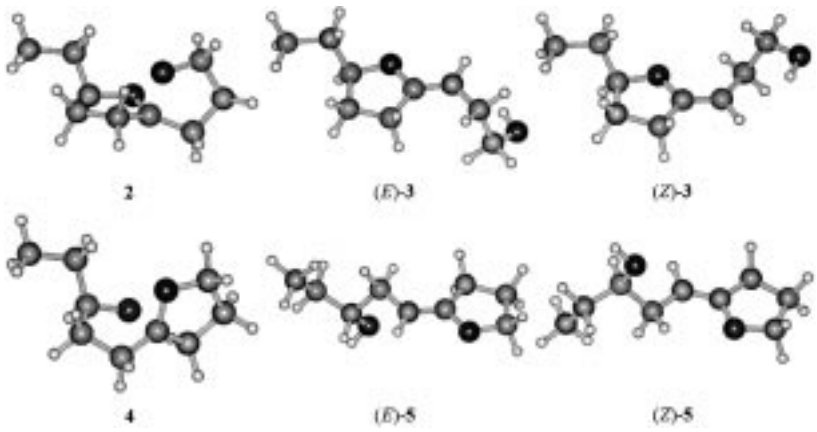

Figure 7. PM3-optimized structures of the intermediates.

Table 4. Absolute and relative energies for (2*R*,5*S*)-**1** from the calculation using the PM3 method.

Structure	Absolute energy E [kJ mol^{-1}]	Relative energy ΔE [kJ mol^{-1}]
(2*R*,5*S*)-**1**	−183609.6	0.0
(2*R*,5*R*)-**1**	−183608.7	0.9
2	−183437.7	171.9
(*E*)-**3**	−183562.0	47.6
(*Z*)-**3**	−183558.1	51.5
4	−183439.5	170.1
(*E*)-**5**	−183554.8	54.8
(*Z*)-**5**	−183550.3	59.3

Experimental Section

The diastereomers of chalcogran **1**, (2*RS*,5*RS*)-2-ethyl-1,6-dioxaspiro[4.4]-nonane, were obtained from Boehringer Ingelheim, Germany. Enantiomerically enriched (2*S*,5*RS*)-**1** was synthesized by alkylation of 2-acetylbutyrolactone with (*S*)-1,2-epoxybutane according to the method of Mori et al.[12b]

Dynamic GC: The separation of **1** into the four stereoisomers was performed on a Carlo Erba Vega gas chromatograph, equipped with a liquid injector (250 °C), a flame-ionization detector (250 °C), and a Shimadzu C-R 6A integrator, employing a fused silica column (50 m × 0.25 mm i.d.) coated with Chirasil-β-Dex[35] (0.3 μm film thickness). Hydrogen was used as carrier gas. The measurements were repeated three times at each temperature from 70 to 120 °C.

Stopped-flow MDGC: Stopped-flow MDGC was performed on a Siemens Sichromat 2 gas chromatograph equipped with two ovens, a pneumatically controlled six-port valve (Valco), a cooling trap in oven 2 for use with liquid nitrogen, a liquid-injector (250 °C), an on-column injector (40 °C) and two flame-ionization detectors (250 °C). The whole process was monitored by a control computer. For separation of **1**, two fused silica columns (column 1 and 3) coated with Chirasil-β-Dex[35] (12.5 m × 0.25 mm i.d., 0.4 μm film thickness, 60 °C) were employed in oven 1. As reaction column 2, a deactivated fused silica column (1 m × 0.25 mm i.d.), coated with polydimethylsiloxane (0.002 μm film thickness) was used. Helium was employed as the inert carrier gas. The measurements were repeated three times at each temperature, with reaction times of 0.5, 1 and 1.5 h to equilibrate the ratio of epimers.

Computer simulation: Simulations of the experimental chromatograms were performed with the program ChromWin,[34b] which is compatible both with the discontinuous plate model and with the stochastic model, running under Windows on an IBM-compatible personal computer. The mobile phase hold-up time t_M (using methane), total retention times t_R, peak half-width ω_h, peak heights h_A and h_B, and the plateau height of the interconverting peaks $h_{plateau}$ were determined experimentally. The initial quantities of the epimers were calculated from the temperature-dependent epimeric ratio, obtained from the stopped-flow MDGC experiment. The adjusting factor for the apparent backward reaction rate k_{-1}^{app} was also calculated from the epimeric ratio [A]/[B] of the stopped-flow MDGC experiment. The simulation was performed for different values of the apparent rate constant k_1^{app} (k_{-1}^{app} being calculated from k_1^{app} according to the principle of microscopic reversibility), using an improved approximation algorithm, in order to find the best agreement of the simulated and experimental elution profiles with the stochastic model plus (SM+) and the theoretical plate model, applying the "Find Barrier of Isomerization II" method of ChromWin. After that the elution profiles were added with the combination tool of ChromWin.

Molecular modeling calculations: Calculations were performed with the HyperChem package, release 4.0. The initial structures were model build and the first energy minimizations were carried out using the MM+ force field. After that, the obtained structure was refined with the semiempirical method PM3, using the standard parameters of the package. All atomic

0947-6539/01/0707-1500 $ 17.50+.50/0 *Chem. Eur. J.* **2001**, *7*, No. 7

positions were optimized with the conjugate gradient method (Polak–Ribiere) until the RMS gradient reached a value of 0.01 kcal $Å^{-1}mol^{-1}$.

For the variation of the torsion angles in 10° steps, a constraint of 10000 kcal mol^{-1} was applied to the atoms O1–C2–C1′–C2′.

For the calculation of the proposed transition states the structures were constrained to a planar sp^2 configuration (10000 kcal mol^{-1}) at the spiro center C5.

Acknowledgements

This work was supported by the Deutsche Forschungsgemeinschaft, Fonds der chemischen Industrie and the Graduiertenkolleg "Chemistry in Interphases". O.T. thanks the Stiftung Stipendien, Fonds der chemischen Industrie for a doctoral scholarship. We are grateful to Boehringer Ingelheim, Germany, for providing us with (2*RS*,5*RS*)-2-ethyl-1,6-dioxaspiro[4.4]nonane.

[1] a) H. Osada, H. Koshino, K. Isono, H. Takahashi, G. Kawanishi, *J. Antibiot.* **1991**, *44*, 259; b) H. Takahashi, H. Osada, H. Koshino, T. Kudo, S. Amano, S. Shimizu, M. Yoshihama, K. Isono, *J. Antibiot.* **1992**, *45*, 1409; c) H. Takashi, H. Osada, H. Koshino, M. Sasaki, R. Onose, M. Nakakoshi, M. Yoshihama, K. Isono, *J. Antibiot.* **1992**, *45*, 1414; d) H. Koshino, H. Takahashi, H. Osada, K. Isono, *J. Antibiot.* **1992**, *45*, 1420; e) H. Takashi, Y. Yamashita, H. Takaoka, J. Nakamura, M. Yoshihama, H. Osada, *Oncology Res.* **1997**, *9*, 7.

[2] K. E. Drouet, E. A. Theodorakis, *Chem. Eur. J.* **2000**, *6*, 1987.

[3] a) D. A. Evans, C. E. Sachs, W. A. Kleschick, T. R. Taber, *J. Am. Chem. Soc.* **1979**, *101*, 6789; b) G. R. Martinez, P. A. Grieco, E. Williams, K. Kanai, C. V. Srinivasan, *J. Am. Chem. Soc.* **1982**, *104*, 1436; c) M. J. Zmijewski, R. Wong, J. W. Paschal, D. E. Dorman, *Tetrahedron* **1983**, *39*, 1255; d) Y. Nakahara, A. Fujita, K. Beppu, T. Ogawa, *Tetrahedron* **1986**, *42*, 6465; e) R. K. Boeckman, A. B. Charette, T. Asberom, B. H. Johnston, *J. Am. Chem. Soc.* **1987**, *109*, 7553; f) D. P. Negri, Y. Kishi, *Tetrahedron Lett.* **1987**, *28*, 1063; g) J.-G. Gourcy, M. Prudhomme, G. Dauphin, G. Jeminet, *Tetrahedron Lett.* **1989**, *30*, 351; h) F. E. Ziegler, W. T. Cain, *J. Org. Chem.* **1989**, *54*, 3347; i) R. K. Boeckman, A. B. Charette, T. Asberom, B. H. Johnston, *J. Am. Chem. Soc.* **1991**, *113*, 5337.

[4] a) G. R. Pettit, M. Inoue, Y. Kamano, C. Dufresne, N. D. Christie, M. L. Niven, D. L. Herald, *J. Chem. Soc. Chem. Commun.* **1988**, 865; b) G. R. Pettit, M. Inoue, Y. Kamano, D. L. Herald, C. Arm, C. Dufresne, N. D., Christie, J. M. Schmidt, D. L. Doubek, T. S. Krupa, *J. Am. Chem. Soc.* **1988**, *110*, 2006.

[5] a) H. E. Kenney, M. E. Wall, *J. Org. Chem.* **1957**, *22*, 468; b) Y. Mazur, N. Danieli, F. Sondheimer, *J. Am. Chem. Soc.* **1960**, *82*, 5889; c) S. B. Makato, N. P. Sahu, A. N. Ganguly, K. Migakara, T. Kawasaki, *J. Chem. Soc. Perkin Trans. I* **1981**, 2405; d) S. Seo, K. Tori, A. Uomori, Y. Yoshimura, *J. Chem. Soc. Chem. Commun.* **1981**, 895.

[6] P. M. Pihko, A. M. P. Koskinen, *J. Org. Chem.* **1998**, *63*, 92.

[7] a) I. Paterson, R. M. Oballa, R. D. Norcross, *Tetrahedron Lett.* **1996**, *37*, 8581; b) I. Paterson, K. R. Gibson, R. M. Oballa, *Tetrahedron Lett.* **1996**, *37*, 8585; c) I. Paterson, L. E. Keown, *Tetrahedron Lett.* **1997**, *38*, 5727; d) I. Patterson, R. M. Oballa, *Tetrahedron Lett.* **1997**, *38*, 8241; e) I. Paterson, D. J. Wallace, K. R. Gibson, *Tetrahedron Lett.* **1997**, *38*, 8911.

[8] B. D. Suthers, M. F. Jacobs, W. Kitching, *Tetrahedron Lett.* **1998**, *39*, 2621.

[9] a) W. Francke, G. Hindorf, W. Reith, *Angew. Chem.* **1978**, *90*, 915; *Angew. Chem. Int. Ed. Engl.* **1978**, *17*, 862; b) W. Francke, W. Reith, G. Bergström, J. Tengö, *Naturwissenschaften* **1980**, *67*, 199; c) R. Baker, R. Herbert, Ph. E. Howse, O. T. Jones, W. Francke, W. Reith, *J. Chem. Soc. Chem. Commun.* **1980**, 52.

[10] W. Francke, V. Heemann, B. Gerken, J. A. A. Renwick, J. P. Vité, *Naturwissenschaften* **1977**, *64*, 590.

[11] a) C. Phillips, R. Jacobson, B. Abrahams, H. J. Williams, L. R. Smith, *J. Org. Chem.* **1980**, *45*, 1920; b) R. E. Ireland, D. Haebich, *Chem. Ber.* **1981**, *114*, 1418; c) R. Jacobson, R. J. Taylor, H. J. Williams, L. R. Smith, *J. Org. Chem.* **1982**, *47*, 3140; d) D. Enders, W. Dahmen, E. Dederichs, P. Weuster, *Synth. Commun.* **1983**, *13*, 1235; e) B. Mudryk, C. A. Shook, T. Cohen, *J. Am. Chem. Soc.* **1990**, *112*, 6389.

[12] a) L. R. Smith, H. J. Williams, R. M. Silverstein, *Tetrahedron Lett.* **1978**, *35*, 3231; b) K. Mori, M. Sasaki, S. Tamada, T. Suguro, S. Masuda, *Tetrahedron* **1979**, *35*, 1601; c) H. Redlich, W. Francke, *Angew. Chem.* **1980**, *92*, 640; *Angew. Chem. Int. Ed. Engl.* **1980**, *19*, 630; d) E. Hungerbuehler, R. Naef, D. Wasmuth, D. Seebach, H.-R. Loosli, A. Wehrli, *Helv. Chim. Acta* **1980**, *63*, 1960; e) H.-E. Hoegberg, E. Hedenstroem, R. Isaksson, A.-B. Wassgren, *Acta Chem. Scand. Ser. B* **1987**, *41*, 694; f) C. Paolucci, C. Mazzini, A. Fava, *J. Org. Chem.* **1995**, *60*, 169.

[13] a) E. L. Plummer, T. E. Stewart, K. Byrne, G. T. Pearce, R. M. Silverstein, *J. Chem. Ecol.* **1976**, *2*, 307; b) J. P. Vité, J. A. A. Renwick, *Z. Angew. Entomol.* **1976**, *82*, 112; c) R. Rossi, *Synthesis* **1978**, 413.

[14] a) K. Mori, *Tetrahedron* **1974**, *30*, 4223; b) D. L. Wood, L. E. Browne, B. Ewing, K. Lindahl, W. D. Bedard, P. E. Tilden, K. Mori, G. B. Pitman, P. R. Hughes, *Science* **1976**, *192*, 896; c) K. Mori, *Tetrahedron* **1975**, *31*, 1381; d) R. Rossi, *Synthesis* **1978**, 413; e) K. Mori, *Chirality* **1989**, *10*, 578; f) E. Dunkelblum, R. Gries, G. Gries, K. Mori, Z. Mendel, *J. Chem. Ecol.* **1995**, *21*, 849; g) S. Kurosawa, M. Takenaka, E. Dunkelblum, Z. Mendel, K. Mori, *ChemBioChem* **2000**, *1*, 56.

[15] K. Mori in *Methods in Chemical Ecology*, *Vol. 1* (Eds.: J. G. Millar, K. F. Haynes), Kluwer, Boston, **1998**, p. 295.

[16] a) B. Koppenhöfer, K. Hintzer, R. Weber, V. Schurig, *Angew. Chem.* **1980**, *92*, 473; *Angew. Chem. Int. Ed. Engl.* **1980**, *19*, 471; b) R. Weber, K. Hintzer, V. Schurig, *Naturwissenschaften* **1980**, *67*, 453; c) R. Weber, V. Schurig, *Naturwissenschaften* **1981**, *68*, 330.

[17] a) V. Schurig, B. Koppenhöfer, W. Bürkle, *Angew. Chem.* **1978**, *90*, 993; *Angew. Chem. Int. Ed. Engl.* **1978**, *17*, 937; b) V. Schurig, W. Bürkle, *J. Am. Chem. Soc.* **1982**, *104*, 7573.

[18] a) V. Schurig, *J. Chromatogr. A* **1988**, *441*, 135; b) S. Allenmark, V. Schurig, *J. Mater. Chem.* **1997**, *7*, 1955.

[19] a) V. Schurig, W. Bürkle, *Angew. Chem.* **1978**, *90*, 132; *Angew. Chem. Int. Ed. Engl.* **1978**, *17*, 132; b) V. Schurig, R. Weber, *J. Chromatogr.* **1984**, *217*, 51; c) V. Schurig, W. Bürkle, K. Hintzer, R. Weber, *J. Chromatogr.* **1989**, *475*, 23.

[20] H.-P. Nowotny, D. Schmalzing, D. Wistuba, V. Schurig, *J. High Res. Chromatogr.* **1989**, *12*, 383.

[21] W. A. König, D. Icheln, T. Runge, I. Pforr, A. Krebs, *J. High Res. Chromatogr.* **1990**, *13*, 702.

[22] V. Schurig in *Chromatographic Separations Based on Molecular Recognition* (Ed.: K. Jinno), Wiley-VCH, New York, **1997**, p. 371.

[23] K. Hintzer, R. Weber, V. Schurig, *Tetrahedron Lett.* **1981**, *22*, 55.

[24] a) P. J. Marriott, Y.-H. Lai, *J. Chromatogr.* **1988**, *447*, 29; b) P. J. Marriott, Y.-H. Lai, *Chem. Aust.* **1994**, *61*, 386.

[25] a) W. Melander, H. Lin, J. Jacobson, C. Horváth, *J. Phys. Chem.* **1984**, *88*, 4527; b) J. Jacobson, W. Melander, G. Vaisnys, C. Horváth, *J. Phys. Chem.* **1984**, *88*, 4536; c) S. Friebe, G.-J. Krauss, H. Nitsche, *J. Chromatogr.* **1992**, *598*, 139; d) S. Friebe, B. Hartrodt, K. Neubert, G.-J. Krauss, *J. Chromatogr. A* **1994**, *661*, 7; e) A. Wutte, G. Gübitz, S. Friebe, G.-J. Krauss, *J. Chromatogr. A* **1994**, *677*, 186; f) A. S. Rathore, C. Horváth, *Electrophoresis* **1997**, *18*, 2935.

[26] Y.-H. Lai, P. J. Marriott, B.-C. Tan, *Aust. J. Chem.* **1985**, *38*, 307.

[27] a) P. J. Marriott, Y.-H. Lai, *Inorg. Chem.* **1986**, *25*, 3680; b) P. C. Uden, Y. Zeng, *Chromatographia* **1992**, *34*, 269.

[28] a) V. Schurig, W. Bürkle, *J. Am. Chem. Soc.* **1982**, *104*, 7573; b) M. Reist, B. Testa, P. A. Carrupt, M. Jung, V. Schurig, *Chirality* **1995**, *7*, 396. In contrast to the irreversible macroscopic process of racemiziation, enantiomerization is defined as the reversible microscopic conversion of one enantiomer into another. In the case of two chiral centers, only epimers and enantiomers exist. In cases of three and more chiral centers "real" diastereomers, epimers and enantiomers occur.

[29] a) E. L. Eliel, S. H. Wilen in *Stereochemistry of Organic Compounds*, 1st ed., Wiley, New York, **1994**, p. 1196; b) G. Helmchen, *Enantiomer* **1996**, *1*, 185, Glossary of Problematic Terms in Organic Stereochemistry. Diastereomerization is defined as the conversion of one diastereomer. Epimerization is a subsidiary item under diastereomerization and describes the change of configuration of a single stereogenic unit.

[30] a) L. C. Craig, *J. Biol. Chem.* **1944**, *155*, 519; b) J. Kallen, E. Heilbronner, *Helv. Chim. Acta* **1960**, *43*, 489; c) W. Bürkle, H. Karfunkel, V. Schurig, *J. Chromatogr.* **1984**, *288*, 1.

[31] A. Mannschreck, H. Zinner, N. Pustet, *Chimia* **1989**, *43*, 165.
[32] a) M. Jung, V. Schurig, *J. Am. Chem. Soc.* **1992**, *114*, 529; b) M. Jung, *Program Simulation*, *No. 620*, *Quantum Chemistry Program Exchange (QCPE)*, *QCPE Bull.* **1992**, *3*, 12.
[33] a) J. Veciana, M. I. Crespo, *Angew. Chem.* **1991**, *103*, 85; *Angew. Chem. Int. Engl. Ed.* **1991**, *30*, 74; b) C. Wolf, W. A. König, C. Roussel, *Liebigs Ann.* **1995**, 781; c) C. Wolf, D. H. Hochmuth, W. A. König, C. Roussel, *Liebigs Ann.* **1996**, 357; d) D. H. Hochmuth, W. A. König, *Liebigs Ann.* **1996**, 947; e) F. Gasparrini, D. Misiti, M. Pierini, C. Villani, *Tetrahedron*: *Asymmetry* **1997**, *8*, 2069; d) J. Oxelbark, S. Allenmark, *J. Org. Chem.* **1999**, *64*, 1483.
[34] a) O. Trapp, V. Schurig, *J. Am. Chem. Soc.* **2000**, *122*, 1424; b) O. Trapp, V. Schurig, *Comput. Chem.* **2001**, *25*, 187; c) G. Schoetz, O. Trapp, V. Schurig, *Anal. Chem.* **2000**, *72*, 2758; d) G. Schoetz, O. Trapp, V. Schurig, *Enantiomer* **2000**, *5*, 391; e) S. Reich, O. Trapp, V. Schurig, *J. Chromatogr. A* **2000**, *892*, 487; f) G. Schoetz, O. Trapp, V. Schurig, *J. High Res. Chromatogr.* **2000**, *23*, 290; g) O. Trapp, V. Schurig, *J. High Res. Chromatogr.* **2000**, *23*, 291.
[35] V. Schurig, D. Schmalzing, M. Schleimer, *Angew. Chem.* **1991**, *103*, 994; *Angew. Chem. Int. Engl. Ed.* **1991**, *30*, 987.
[36] H. A. Keller, J. C. Giddings, *J. Chromatogr.* **1960**, *3*, 205.
[37] a) R. Kramer, *J. Chromatogr.* **1975**, *107*, 241; b) E. Cremer, R. Kramer, *J. Chromatogr.* **1975**, *107*, 253.
[38] a) V. Schurig, S. Reich, *Chirality* **1998**, *10*, 316; b) R. G. Kostyanovsky, G. K. Kadorkina, V. R. Kostyanovsky, V. Schurig, O. Trapp, *Angew. Chem.* **2000**, *112*, 3066; *Angew. Chem. Int. Ed.* **2000**, *39*, 2938.
[39] F. R. Gonzales, *J. Chromatogr. A* **1999**, *832*, 165.
[40] a) A. A. Frost, R. G. Pearson in *Kinetics Mechanism*, 2nd ed., Wiley, New York, **1961**, p. 135; b) H. Hermann, R. Huisgen, H. Mader, *J. Am. Chem. Soc.* **1971**, *93*, 1779; c) E. W. Yankee, F. D. Bader, N. E. Howe, D. J. Cram, *J. Am. Chem. Soc.* **1973**, *95*, 4210; d) O. Gonzales, D. E. Gallis, D. R. Crist, *J. Org. Chem.* **1986**, *51*, 3266.
[41] a) H.-D. Beckhaus, G. Hellmann, C. Rüchardt, *Chem. Ber.* **1978**, *111*, 72; b) A. Haas, K. Schlosser, S. Steenken, *J. Am. Chem. Soc.* **1979**, *101*, 6282; c) K. Schlosser, S. Steenken, *J. Am. Chem. Soc.* **1983**, *105*, 1504.
[42] a) B. Stephan, H. Zinner, F. Kastner, A. Mannschreck, *Chimia* **1990**, *10*, 336; b) L. Loncar-Tomascovic, K. Lorenz, A. Hergold-Brundic, D. Mrvos-Sermek, A. Nagl, M. Mintas, A. Mannschreck, *Chirality* **1999**, *11*, 363.
[43] K. Lorenz, E. Yashima, Y. Okamoto, *Angew. Chem.* **1998**, *110*, 2025; *Angew. Chem. Int. Ed.* **1998**, *37*, 1922.
[44] HyperChem release 4.0 and ChemPlus release 1.5, available from Hypercube Inc., 1115 NW 4th Street, Gainesville, FL 32601-4256, USA.
[45] N. L. Allinger, *J. Am. Chem. Soc.* **1977**, *99*, 8127.
[46] a) M. J. S. Dewar, E. G. Zoebisch, E. F. Healy, J. J. P. Stewart, *J. Am. Chem. Soc.* **1985**, *107*, 3902; b) M. J. S. Dewar, K. M. Dieter, *J. Am. Chem. Soc.* **1986**, *108*, 8075; c) J. J. P. Stewart, *J. Comput. Chem.* **1989**, *10*, 209; d) J. J. P. Stewart, *J. Comput. Chem.* **1989**, *10*, 221; e) J. J. P. Stewart, *J. Comp. Aided Mol. Design* **1990**, *4*, 1; f) J. J. P. Stewart in *Reviews of Computational Chemistry* (Eds.: K. Lipkowitz, D. B. Boyd), VCH, New York, **1990**, p. 45.

Received: August 18, 2000 [F2684]

  0947-6539/01/0707-1502 $ 17.50+.50/0